

RADIO IDENTIFICATION OF THE X-RAY JET IN THE Z=4.3 QUASAR GB 1508+5714

C. C. CHEUNG

Department of Physics, MS 057, Brandeis University, Waltham, MA 02454

ccheung@brandeis.edu

ApJL, accepted

ABSTRACT

The recent discovery of an X-ray jet in the $z=4.3$ quasar GB 1508+5714 by Yuan et al. (astro-ph/0309318) and Siemiginowska et al. (astro-ph/0310241) prompted a search for its radio counterpart. Here, we report the successful discovery of faint radio emission from the jet at 1.4 GHz using archival VLA data. The X-ray emission is best interpreted as inverse Compton (IC) emission off the CMB as discussed by the previous investigators. In this scenario, its high X-ray to radio monochromatic luminosity ratio, compared to previously detected IC/CMB X-ray jets at lower redshift, is a natural consequence of its high redshift.

Subject headings: Galaxies: active — galaxies: jets — quasars: general — quasars: individual (GB 1508+5714) — radio continuum: galaxies — X-rays: galaxies

1. BACKGROUND

Since its launch in 1999, the Chandra X-ray Observatory has been used to detect a large number of X-ray jets in Active Galactic Nuclei (AGN), where prominent radio jets were previously known to exist (see e.g., Harris & Krawczynski 2002, and associated website¹). The recent report (Yuan et al. 2003; Siemiginowska et al. 2003b) of an extended X-ray jet originating from the $z=4.3$ quasar GB 1508+5714, where previous observations showed no obvious sign of extended radio emission, presents an interesting case. The X-ray feature is strong – well over 100 counts were detected from it in the ~ 90 ksec Chandra exposure. An archival HST image helps rule out the possibility that it is due to a foreground galaxy or a gravitationally lensed image of the quasar (Siemiginowska et al. 2003b). Based on deep X-ray source counts, it has a low probability of being a random unassociated X-ray field source.

As discussed by the previous authors, such detections of X-ray jets at large redshifts are actually to be expected as a natural consequence of the inverse Compton (IC) off the CMB model (e.g., Tavecchio et al. 2000; Celotti, Ghisellini, & Chiaberge 2001). This is because the $(1+z)^4$ dependence of the CMB energy density compensates for cosmological dimming of radiation, so that IC/CMB X-ray jets should remain detectable out to large cosmological distances (Schwartz 2002a). The model has been successfully applied to account for X-ray jets in many other powerful quasars at more modest redshifts (e.g., Sambruna et al. 2002), requiring that the jets are still highly relativistic on kilo-parsec scales, in order that the electrons in the jet frame see an adequately boosted photon source. However, the lack of a detection of the GB 1508+5714 jet at lower frequencies, along with only a rough constraint on the X-ray spectrum, could not rule out a synchrotron origin for the X-rays (Siemiginowska et al. 2003b). A previous search in the radio for a proposed X-ray jet in another high redshift ($z=5.99$) quasar, SDSS 1306+0356 (Schwartz 2002b), yielded only an upper limit of <0.1 mJy at 1.4 GHz (Petric et al. 2003; Schwartz, Cheung, & Wardle 2003).

Distinguishing between the two possible emission processes is important, as they probe different energetic phenomena. In

the case of synchrotron X-ray emission, the X-rays mark sites of particle acceleration with electrons accelerated up to $\gamma \sim 10^7$ with very short lifetimes (e.g. M87; Harris et al. 2003). When considered together with minimum energy/equipartition conditions, the IC/CMB model offers important constraints on the beaming, magnetic field, and jet power (Tavecchio et al. 2000; Celotti, Ghisellini, & Chiaberge 2001).

Both the IC and synchrotron interpretations of X-ray jet emission usually require a population of relativistic electrons emitting synchrotron radiation at lower (radio) frequencies. Based on the X-ray flux and spectrum, the two models give different predictions of the radio component flux and spectrum. Here, we report the detection of such a radio component coincident with the X-ray feature extending from GB 1508+5714 from an analysis of archival VLA data. This supports its interpretation as an X-ray jet and we discuss the X-ray emission in the context of the new 1.4 GHz detection, along with the previously set optical, and a new 8.4 GHz limit. Following Yuan et al. (2003) and Siemiginowska et al. (2003b), $H_0 = 71$ km s⁻¹ Mpc⁻¹, $\Omega_M = 0.27$ and $\Omega_{vac} = 0.73$ (Spergel et al. 2003) are assumed throughout, so $1'' = 6.871$ kpc.

2. ARCHIVAL RADIO OBSERVATIONS

Two datasets which utilized the VLA in its highest resolution A-configuration were obtained from the NRAO² archive. The data were calibrated in the NRAO AIPS package (Bridle & Greisen 1994) and brought into DIFMAP (Shepherd, Pearson, & Taylor 1994) for editing, self-calibration, and imaging. The flux density scale was set on the VLA 1999.2 scale using scans of 3C 286 as outlined in the VLA Calibrator Manual (Perley & Taylor 2003).

The 1.4 GHz dataset – a single five minute snapshot observation – yielded a 10σ detection of a 1.2 mJy feature extended from the quasar (Figure 1). This feature is only about 0.5% of the core flux ($224 \pm 5\%$ mJy), so it is no surprise that the original investigators (Moran & Helfand 1997) simply concluded that the quasar was an unresolved point source from these data. The measured off-source RMS of $\lesssim 0.12$ mJy in the image is within 50% of the thermal noise limit expected from the integration time. The resultant image has a dynamic range of

¹ <http://hea-www.harvard.edu/XJET/>

² The National Radio Astronomy Observatory is a facility of the National Science Foundation operated under cooperative agreement by Associated Universities, Inc.

almost 2,000:1.

The jet knot was modeled with an elliptical gaussian profile in both the (u,v) plane with DIFMAP's MODELFIT utility, and in the map plane with the JMFIT task in AIPS. The fits gave consistent measures of the deconvolved size: $1'' \times < 1''$, elongated along the jet direction. We note that this is comparable to the beamsize for this observation so the source is consistent with being unresolved, and the size should be considered an upper limit. The separation from the core is $2.5''$ at a position angle of -114° , and is comparable to that measured from the X-ray data. Interestingly however, the peak in the X-ray jet appears somewhat closer to the nucleus than the radio centroid in the image overlay (Figure 2), by about one Chandra ACIS pixel ($0.492''$ per pixel), or equivalently ~ 3 kpc projected distance. The images were aligned by the cores to better than half of a pixel. Siemiginowska et al. (2003b) found the peak in the X-ray jet to be $\sim 2''$ away (see also their subpixel re-binned radial profile published in their Figure 2), consistent with our qualitative assessment. Yuan et al. (2003) stated the same peak to be $\sim 3''$ distant from the nucleus, although we measured a smaller value off their Figure 1. Much more apparent X-ray/radio offsets are seen in other powerful quasars (e.g. up to $\sim 2''$ in PKS 1127–145; Siemiginowska et al. 2002). Most, if not all of the X-ray counts from the GB 1508+5714 jet lie within the outermost radio contour in the VLA image (Figure 2).

A 10-minute 8.4 GHz observation obtained on Nov 3, 1996 (Program AD388) yielded no detection of the radio jet. The measured off-source RMS in the naturally weighted image ($\sim 0.35''$ beam) is at about the expected thermal noise limit of 0.045 mJy. In order to judge if the non-detection was a result of the greater resolution in this image compared to the 1.4 GHz map, the 8.4 GHz dataset were tapered by different amounts. No outstanding feature appeared above the residual artifacts from the dirty beam. The measured RMS at the expected position of the jet in a tapered image restored with a $0.75''$ beam is 0.3 mJy (3σ). This, along with the 1.4 GHz detection, is consistent with an $\alpha \gtrsim 0.8$ radio spectrum ($F_\nu \propto \nu^{-\alpha}$), which agrees with the measured X-ray spectral index: 0.9 ± 0.36 (Siemiginowska et al. 2003b) and $0.92^{+0.38}_{-0.33}$ (Yuan et al. 2003).

3. CONSTRAINTS FROM THE RADIO DATA

The spectral energy distribution of the jet knot in GB 1508+5714 is shown in Figure 3. If the X-ray and radio emission are drawn from the same population of relativistic electrons emitting synchrotron radiation, the spectral index will be about what is measured between the 1.4 GHz and X-ray (using 1.68×10^{-6} ph/cm²/s/keV at 1 keV, reported by Siemiginowska et al. (2003b)) detections: $\alpha_{\text{rx}} = 0.73$. This is a typical value for the spectrum seen in radio jets (Bridle & Perley 1984), and is consistent with the measured X-ray spectrum of $\simeq 0.9 \pm 0.36$ (Yuan et al. 2003; Siemiginowska et al. 2003b), and our constraint on the radio spectrum of $\gtrsim 0.8$ (the modest 8.4 GHz dataset does not preclude that the higher frequency radio emission, >40 GHz in the source frame, was actually resolved out). The optical HST limit (3σ) from Siemiginowska et al. (2003b) is not useful in this case, as it hovers over the radio-to-X-ray spectrum, and only weaker constraints are available at other optical bands (Yuan et al. 2003).

We can estimate an equipartition magnetic field of $B_{\text{eq}} \simeq 9.7 \times 10^{-5} \delta^{-1} \gamma_{\text{min}}^{-0.12} (\eta / f)^{0.27}$ G, by adopting the observed α_{rx} value as the optically thin spectral index, and that the particles and field fill a fraction f of a 2.9×10^{67} cm³ sphere, correspond-

ing to the size upper limit derived from the radio detection. The factor η is the ratio of magnetic field and electron energy densities, and γ_{min} is the lower energy cutoff of a power law distribution of relativistic particles. If we further assume $\eta=1$, $f=1$, and $\gamma_{\text{min}}=10$, then $B_{\text{eq}} \simeq 7.4 \times 10^{-5} \delta^{-1}$ G, where δ is the unknown jet Doppler beaming factor. In this field, electrons emitting the highest energy X-rays detected (~ 5 keV; Siemiginowska et al. 2003b) will have $\gamma \sim 10^8$ and short lifetimes (~ 50 years) – this would require continuous in-situ reacceleration of high energy particles in order that the X-ray jet not be a transient feature. At this high redshift, the energy density of the CMB already exceeds that of the equipartition field, even without bulk motion (see below), so inverse Compton losses will already be dominant. The lifetime of the $\gamma \sim 10^8$ electrons calculated above is then a strict upper limit. Taking this evidence together, it is unlikely that the jet X-ray emission is dominated by synchrotron losses.

An IC/CMB origin for this high redshift X-ray jet is preferred (Yuan et al. 2003; Siemiginowska et al. 2003b), and give us an additional constraint on the allowed range of magnetic field and jet Doppler factor to the equipartition condition. The following expression is taken from Tavecchio (2002):

$$B = \delta \left[\frac{3}{2} \frac{c(\alpha)}{\sigma_T c} \frac{1}{U_{\text{rad}}} \frac{\nu_c^\alpha F_c(\nu_c)}{\nu_s^\alpha F_s(\nu_s)} \right]^{-1/(1+\alpha)}, \quad (1)$$

where, $c(\alpha)$ is a dimensionless function of α (e.g., Ghisellini, Maraschi, & Treves 1985), σ_T is the Thomson cross section, and $U_{\text{rad}} = 4.19 \times 10^{-13} (1+z)^4$ ergs cm⁻³ for the CMB (e.g., Schwartz 2002a), whose spectrum is peaked near $\nu_0 = 1.6 \times 10^{11} (1+z)$ Hz (Harris & Krawczynski 2002). Assuming $\alpha = 1$, the observed ratio of the Compton (X-ray) and synchrotron (radio) fluxes (F_c and F_s , observed at ν_c and ν_s , respectively), allow us to estimate $B \simeq 7.2 \times 10^{-6} \delta$ G. The corresponding equipartition calculation gives $B_{\text{eq}} \simeq 10^{-4} \delta^{-1}$ G, making the assumptions as above about η , f , and γ_{min} . Both estimates of B -field are reasonably insensitive to the assumed spectral index: up to $\sim 25\%$ smaller for $\alpha = 0.9$, the measured X-ray spectral index. In order to reconcile the differences between the two equations (opposite dependencies of B on δ), a Doppler factor greater than one is required. These two constraints bracket a plausible range of solutions around a $30 \mu\text{G}$ field and $\delta \sim 4$. Siemiginowska et al. (2003b) arrived at similar conditions using slightly different assumptions. The unresolved nucleus is a variable X-ray and (flat spectrum) radio source with a very high X-ray to optical luminosity (see, Moran & Helfand 1997, and references therein). These observations have been taken as evidence of beaming on smaller scales, in the nucleus.

The ratio of the monochromatic X-ray to radio luminosities (i.e., in νF_ν) of the GB 1508+5714 jet is 158. This is one of the highest amongst the known X-ray jets which can be attributed to IC/CMB emission so far. In Figure 4, this ratio is plotted vs. redshift along with IC/CMB X-ray jets taken from the literature. The values seem to vary widely over 4 orders of magnitude, but predominantly show X-ray to radio ratios greater than 1. The jet in GB 1508+5714 sees 1–2 orders of magnitude times greater energy density from the CMB than other jets at lower redshift, so it is tempting to speculate that its extreme redshift may account, to first order, for its large X-ray to radio luminosity ratio. This could similarly, account for the large X-ray to radio ratio limit obtained for the proposed X-ray jet in the $z=5.99$ quasar SDSS 1306+0356 (Schwartz 2002b; Schwartz, Cheung, & Wardle 2003, Fig. 4).

The observed monochromatic X-ray to radio luminosity ratios can be compared to what is expected in the IC/CMB model. We can obtain an expression for the expected ratio by rearranging equation 1 (and setting $\alpha = 1$):

$$\frac{\nu_c F_c(\nu_c)}{\nu_s F_s(\nu_s)} = \frac{4.19 \times 10^{-13}(1+z)^4}{(B/\delta)^2/8\pi}. \quad (2)$$

The flux ratio is simply proportional to the ratio of the energy densities in the CMB and magnetic field, with a Doppler factor term. This expression is plotted in Figure 4 for several different combinations of B and δ , one of which, best suits the observations of GB 1508+5714. It appears that varying B and δ can account for the large spread of observed X-ray to radio luminosity ratios within a given redshift range. Larger B -field, or more likely, smaller δ may account for the low values observed in Q0957+561 ($z=1.41$, Chartas et al. 2002) and 3C 9 ($z=2.012$, Fabian, Celotti, & Johnstone 2003), as they are known to have low radio core dominance, and weak VLBI structures (Campbell et al. 1995; Hough et al. 2002) compared to the other sources studied here. In all but 3C 179 ($z=0.846$, Sambruna et al. 2002) where multiple knot regions along the jet can be distinguished, the X-ray to radio flux ratio decreases with increas-

ing distance from the nucleus, and can similarly be accounted for by varying B/δ . As discussed specifically in the case of 3C 273 ($z=0.158$, Sambruna et al. 2001), the variations along the jet may indicate deceleration, or increasing B along the jet, possibly by compression in strong shocks. Future detections in the redshift range $\sim 2-4$ or higher with large X-ray/radio flux ratios can lend further support to the currently preferred IC/CMB model used to explain the X-ray emission in quasar jets.

An anonymous referee is thanked for making the point that Compton losses are already dominant in the synchrotron X-ray case, and several other useful comments. The author is grateful to John Wardle for his advice and encouragement throughout the course of this work, and to Dan Harris, Aneta Siemiginowska, Dave Roberts, and Fabrizio Tavecchio for useful discussions. Radio astronomy at Brandeis University is supported by the National Science Foundation through grants AST 98-02708 and AST 00-98608. Additional support by NASA grant GO2-3195C from the Smithsonian Astrophysical Observatory, and HST-GO-09122.08-A from the Space Telescope Science Institute, which is operated by AURA, Inc., under NASA contract NAS 5-26555 is acknowledged.

REFERENCES

- Bridle, A. H. & Perley, R. A. 1984, *ARA&A*, 22, 319
 Bridle, A. H. & Greisen, E. W. 1994, AIPS Memo 87 (NRAO: Charlottesville)
 Bridle, A. H., Hough, D. H., Lonsdale, C. J., Burns, J. O., & Laing, R. A. 1994, *AJ*, 108, 766
 Brunetti, G., Bondi, M., Comastri, A., & Setti, G. 2002, *A&A*, 381, 795
 Campbell, R. M., Lehar, J., Corey, B. E., Shapiro, I. I., & Falco, E. E. 1995, *AJ*, 110, 2566
 Celotti, A., Ghisellini, G., & Chiaberge, M. 2001, *MNRAS*, 321, L1
 Chartas, G. et al. 2000, *ApJ*, 542, 655
 Chartas, G., Gupta, V., Garmire, G., Jones, C., Falco, E. E., Shapiro, I. I., & Tavecchio, F. 2002, *ApJ*, 565, 96
 Fabian, A. C., Celotti, A., & Johnstone, R. M. 2003, *MNRAS*, 338, L7
 Ghisellini, G., Maraschi, L., & Treves, A. 1985, *A&A*, 146, 204
 Harris, D. E. & Krawczynski, H. 2002, *ApJ*, 565, 244
 Harris, D. E., Biretta, J. A., Junor, W., Perlman, E. S., Sparks, W. B., & Wilson, A. S. 2003, *ApJ*, 586, L41
 Hough, D. H., Vermeulen, R. C., Readhead, A. C. S., Cross, L. L., Barth, E. L., Yu, L. H., Beyer, P. J., & Phifer, E. M. 2002, *AJ*, 123, 1258
 Moran, E. C. & Helfand, D. J. 1997, *ApJ*, 484, L95
 Perley, R. A., & Taylor, G. B. 2003, VLA Calibrator Manual, NRAO
 Petric, A. O., Carilli, C. L., Bertoldi, F., Fan, X., Cox, P., Strauss, M. A., Omont, A., & Schneider, D. P. 2003, *AJ*, 126, 15
 Sambruna, R. M., Urry, C. M., Tavecchio, F., Maraschi, L., Scarpa, R., Chartas, G., & Muxlow, T. 2001, *ApJ*, 549, L161
 Sambruna, R. M., Maraschi, L., Tavecchio, F., Urry, C. M., Cheung, C. C., Chartas, G., Scarpa, R., & Gambill, J. K. 2002, *ApJ*, 571, 206
 Schwartz, D. A. 2002a, *ApJ*, 569, L23
 Schwartz, D. A. 2002b, *ApJ*, 571, L71
 Schwartz, D. A., Cheung, C. C., & Wardle, J. F. C. 2003, in *Active Galactic Nuclei: from Central Engine to Host Galaxy*, eds. S. Collin, F. Combes, & I. Shlosman, ASP Conf. Series 290, 619
 Shepherd, M. C., Pearson, T. J., & Taylor, G. B. 1994, *BAAS*, 26, 987
 Siemiginowska, A., Bechtold, J., Aldcroft, T. L., Elvis, M., Harris, D. E., & Dobrzycki, A. 2002, *ApJ*, 570, 543
 Siemiginowska, A., Stanghellini, C., Brunetti, G., Fiore, F., Aldcroft, T. L., Bechtold, J., Elvis, M., Murray, S. S., Antonelli, L. A., & Colafrancesco, S. 2003a, *ApJ*, 595, 643
 Siemiginowska, A., Smith, R. K., Aldcroft, T. L., Schwartz, D. A., Paerels, F., and Petric, A. O. 2003b, *ApJL*, accepted (astro-ph/0310241)
 Spergel, D. N. et al. 2003, *ApJS*, 148, 175
 Tavecchio, F., Maraschi, L., Sambruna, R. M., & Urry, C. M. 2000, *ApJ*, 544, L23
 Tavecchio, F. 2002, Ph.D. Thesis, University of Milan
 Yuan, W., Fabian, A. C., Celotti, A., Jonker, P. G. 2003, *MNRAS*, accepted (astro-ph/0309318)

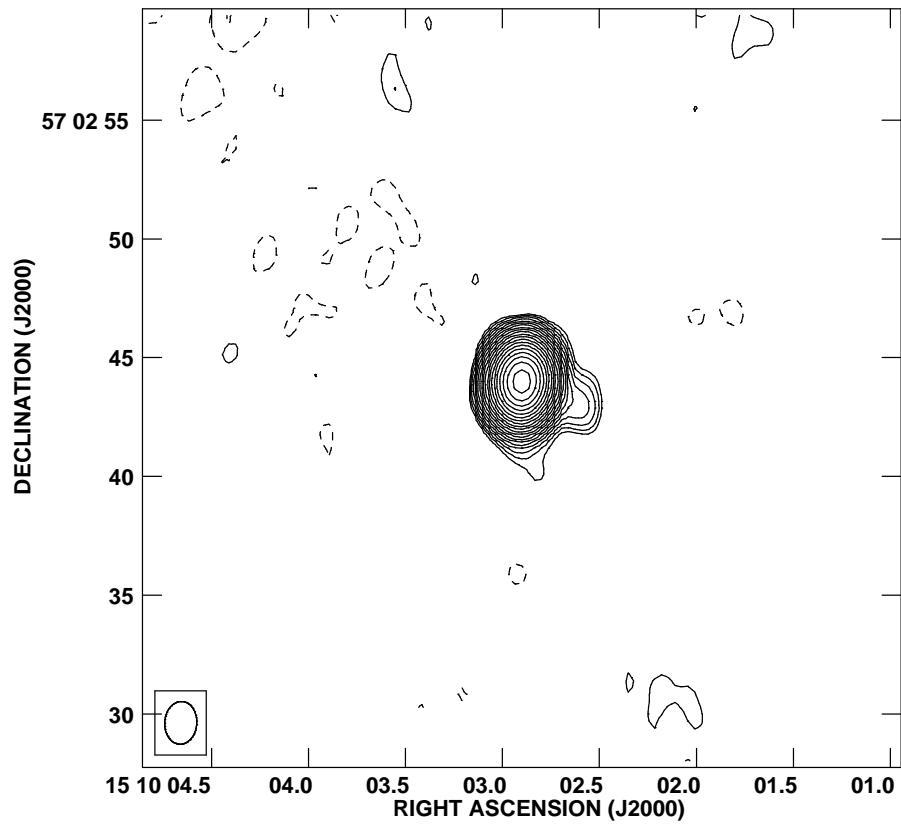


FIG. 1.— Naturally weighted VLA 1.4 GHz archival snapshot image of GB 1508+5714 (at center) and its $\sim 2.5''$ long radio jet extending south of west of the quasar. The contours begin at 0.25 mJy/beam (2 times the measured RMS in the image) and the positive values (solid contours) are spaced by factors of $\sqrt{2}$, with an image peak of 224 mJy/beam. The restoring beam is plotted at the bottom left corner and has dimensions $1.8'' \times 1.35''$ at a position angle of -3.61° .

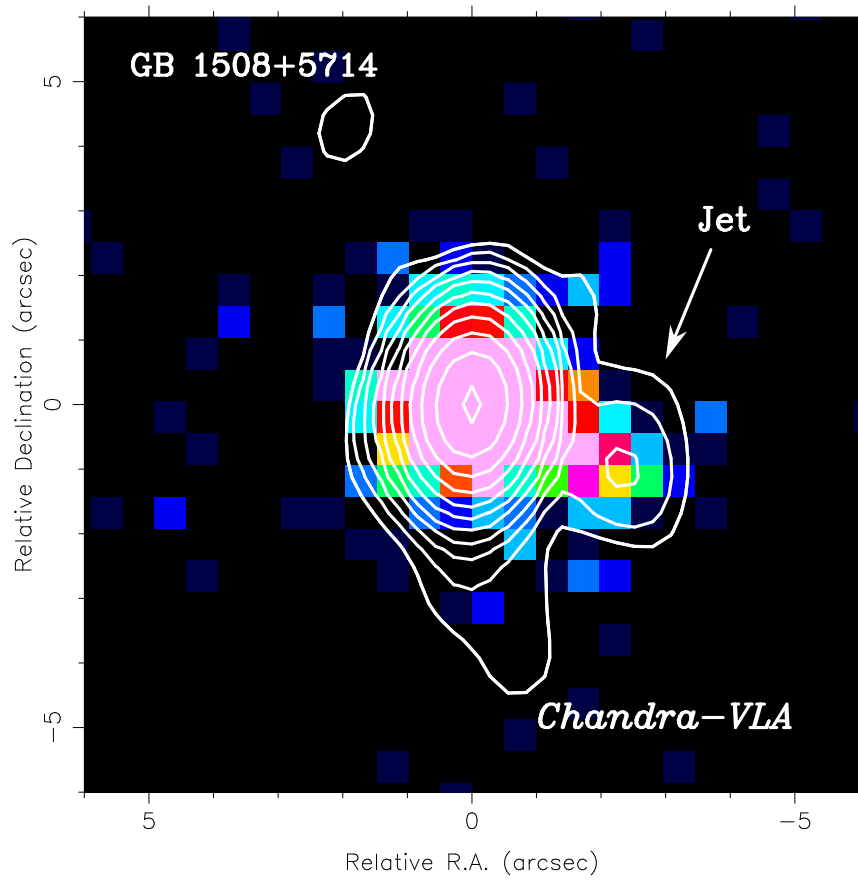


FIG. 2.— Chandra X-ray image of GB 1508+5714 (color) from the archive data published in Yuan et al. (2003) and Siemiginowska et al. (2003b), with VLA 1.4 GHz image overlaid. The quasar is at the origin, and the jet feature indicated. The radio image is from the same data presented in Figure 1 but restored with the uniformly weighted beam ($1.52'' \times 1.03''$ at $PA=-4.44^\circ$). The lowest contour plotted is 0.2 mJy/beam and subsequently spaced by factors of two.

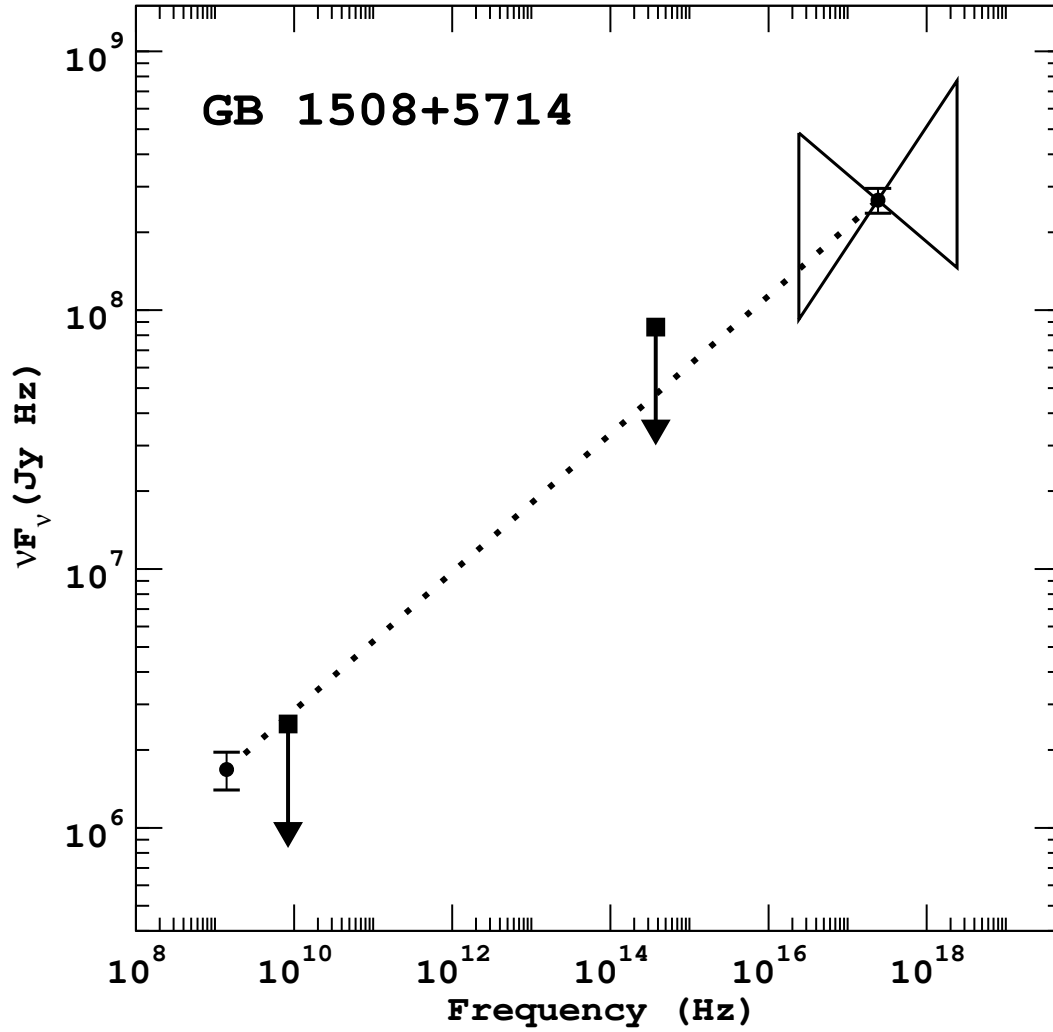


FIG. 3.— Radio-to-X-ray spectral energy distribution of the GB 1508+5714 jet. The bowtie indicates the X-ray spectrum measurement with 1σ uncertainty from Siemiginowska et al. (2003b) and the arrows indicate 3σ limits. The radio data are from this work, and the X-ray point and optical limit were taken from Siemiginowska et al. (2003b). A dotted line shows the α_{rx} slope and simply joins the radio and X-ray detections.

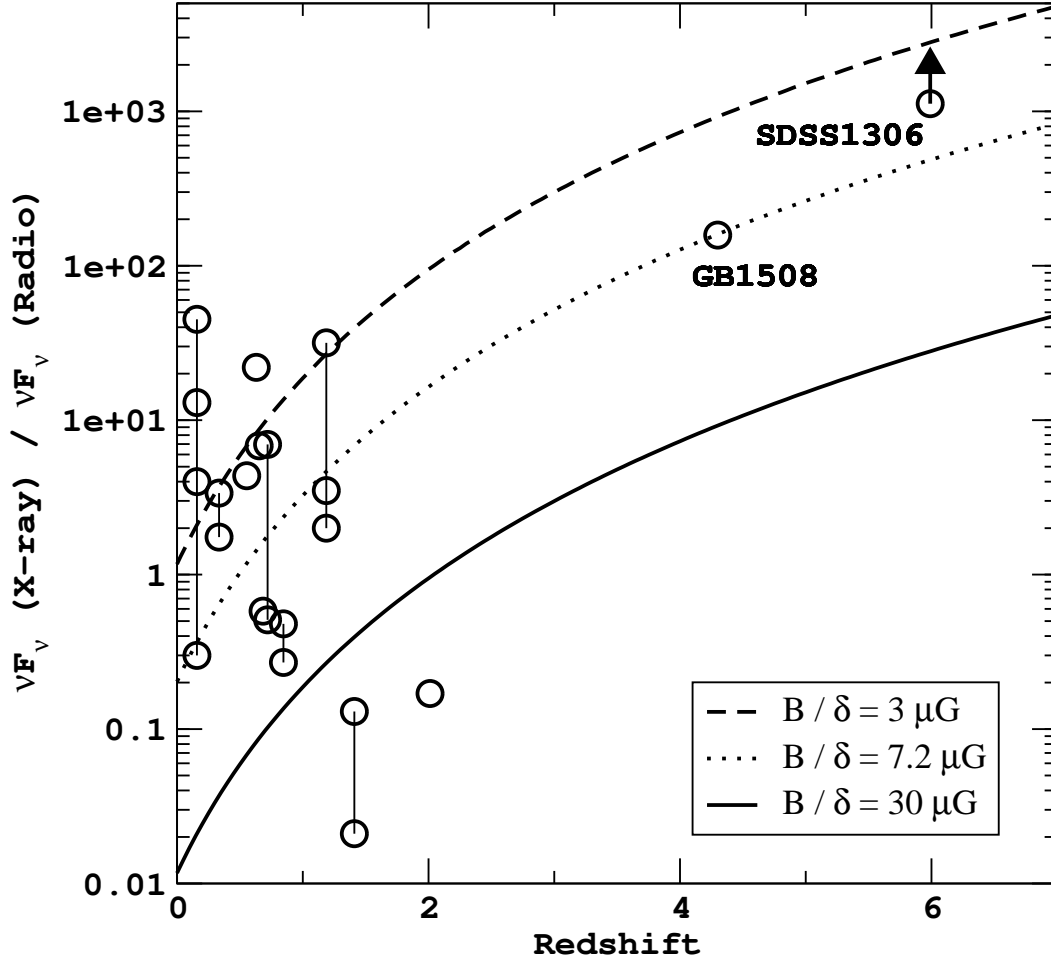


FIG. 4.— Plot of the ratio of the jet X-ray to radio monochromatic luminosity vs. redshift. Only jet features interpreted by the authors as IC/CMB X-ray emission are plotted. The curves indicate the expected ratio for given combinations of B and δ , which scale as $(1+z)^4$. For reference, the $B \sim 30 \mu\text{G}$ and $\delta \sim 4$ case derived for GB 1508+5714, which used the additional equipartition constraint, defines the dotted line which lies in between the other two curves. Light vertical lines connect features from the same source. The data are for (in order of increasing redshift) 3C 273-A to D (Sambruna et al. 2001), 1150+497-A, B, PKS 1136–135-B (Sambruna et al. 2002), B2 0738+313-A (Siemiginowska et al. 2003a), PKS 0637–752-WK7.8 (Chartas et al. 2000), 3C 207-knot (Brunetti et al. 2002), PKS 1354+195-A, B, 3C 179-A, B (Sambruna et al. 2002), PKS 1127–145-A to C (Siemiginowska et al. 2002), Q0957+561-B, C (Chartas et al. 2002), 3C 9-jet (Fabian, Celotti, & Johnstone 2003) with the corresponding radio flux (sum of knots F to J) taken from Bridle et al. (1994), and GB 1508+5714 and SDSS 1306+0356 (see text).